Defect Chemistry of Barium Monoferrite, $BaFe_2O_{4-\delta}$

Akio NAKAMURA,* Shigeru YAMAUCHI, Kazuo FUEKI, and Takashi MUKAIBO

Department of Industrial Chemistry, Faculty of Engineering, The University of Tokyo, Hongo, Bunkyo-ku, Tokyo 113

(Received August 16, 1977)

In order to obtain information on the defects in ternary oxide systems, the nonstoichiometry and electrical conductivity of $BaFe_2O_4$ were determined at temperatures between 1050 and 1125 °C. The electrical conductivity was found to be proportional to $P_{O_2}^{-1/6}$. This relationship suggests that $BaFe_2O_4$ is an oxygen deficient n-type semiconductor at high temperatures. The nonstoichiometry was proportional to $P_{O_2}^{-1/2.88}$. In order to interpret the dependence of electrical conductivity and nonstoichiometry on the oxygen partial pressure, various defect models were examined. As a result the following equilibria were selected from among the oxygen vacancies $V_O^{\cdot\cdot}$ and V_O^{x}, and oxygen gas.

$$\text{null} = (1/2)O_2 + V_O^{x}$$
$$V_O^{x} = V_O^{\cdot\cdot} + 2e'$$

An analysis based on the above defect model explains the data well.

The defect chemistry of oxides is important for the elucidation of transport-phenomena mechanisms, such as electrical conduction, diffusion, metal oxidation, sintering and the other processes for fabricating ceramic materials and heterogeneous catalysts. Although extensive research has been carried out on point defects in simple oxides,[1-3] few studies on defects in complex oxides have been published. Most of the ternary oxide systems studied so far are spinels and perovskite-structure oxides.[4-6] In order to obtain more information about defects in ternary oxide systems of other types of crystal structure, an investigation of the nonstoichiometry δ and the electrical conductivity σ of $BaFe_2O_{4-\delta}$ of stuffed tridymite structure was carried out.

Experimental

Materials. Reagent-grade barium carbonate and hematite of 99.99% purity were mixed in a ratio of Ba/Fe= 1/2. The mixture was cold-pressed into pellets and fired in air at 1100 °C for 12 h to form barium ferrite. One of the sintered pellets was ground and the powder was cold pressed. Then, it was heated again to 1300 °C for 6 h and examined using the X-ray powder diffraction method. The powder was found to consist of β'-$BaFe_2O_4$, a low-temperature modification of barium monoferrite.[7]

The sintered pellets were crushed to grains of 1—2 mm in diameter and used as the sample for the nonstoichiometric measurements. The sintered rectangular specimen, 2× 1.5× 15 mm, was used for the mesurement of the electrical conductivity. The relative density was 88%.

Measurements. The nonstoichiometry of $BaFe_2O_{4-\delta}$ was determined gravimetrically by means of a Shimadzu RMB-50 micro balance at temperatures between 1050 and 1125 °C. The sensitivity of the balance was 1 μg. Details of the equipment have been described elesewhere.[8]

About one gram of the sample was placed in a platinum basket, which was then suspended from the balance by fine alumina fibers. The nonstoichiometry δ was assumed to be zero in 1 atm of oxygen since almost no weight change was observed even when the oxygen pressure was changed from 1 to 0.01 atm at constant temperature. The nonstoichiometry was calculated from the difference in the sample weight in CO_2–CO gas mixtures and in 1 atm of oxygen.

The electrical conductivity was measured using the d.c. four-probe method. Four platinum wires were connected to the sample using platinum paste. Details of the equipment and experimental procedure have been described elsewhere.[9]

Results and Discussion

Nonstoichiometry. A plot of log δ against log P_{O_2} is presented in Fig. 1. The linear relationship between log δ and log P_{O_2} indicate that δ is proportional to $P_{O_2}^{-1/m}$. The values of m calculated from the slope are

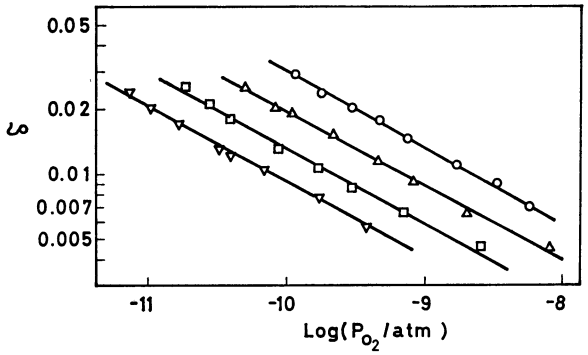

Fig. 1. Dependence of nonstoichiometry δ in $BaFe_2O_{4-\delta}$ on oxygen partial pressure.
▽: 1050 °C, □: 1075 °C, △: 1100 °C, ○: 1125 °C.
The symbols for identification of the temperature is the same through Figs. 1 to 4.

Table 1. Summary of the powers of P_{O_2} from the nonstoichiometric and electric conductivity data

t/°C	m[a]	m'[b]
1050	2.88±0.02[c]	6.6±0.1
1075	2.85±0.03	6.2±0.1
1100	2.85±0.01	6.0±0.05
1125	2.95±0.01	5.5±0.1

a) m is from $\delta \propto P_{O_2}^{-1/m}$. b) m' is from $\sigma \propto P_{O_2}^{-1/m'}$.
c) The errors indicated are for one standard deviation.

*Present address: Research and Development Laboratory TDK Electronics Corporation, 15-7, Higashi Owada 2-Chome, Ichikawa, Chiba 272-01.

given in the second column of Table 1. The mean value of m is 2.88. If the chemical potential of the oxygen atom in the oxide is expressed as

$$\mu_0 = \mu_0^\circ + \frac{1}{2}RT\ln P_{O_2}, \quad (1)$$

the relative partial molar enthalpy of the oxygen atom at a constant composition is given by

$$\Delta H_0^\circ = \partial\left(\frac{1}{2}RT\ln P_{O_2}\right)\Big/\partial(1/T).$$

The ΔH_0° values for $BaFe_2O_{4-\delta}$ are listed in the second column of Table 2. ΔH_0° increases slightly with increasing δ.

Table 2. Partial molar enthalpy of the oxygen atom and the activation energy for electrical conductivity

δ	ΔH_0° / kcal mol^{-1}	ΔH_A / kcal mol^{-1}
0.006	77.1±4.6	12.04±2.66
0.010	77.9±3.0	13.12±1.68
0.012	79.0±3.0	11.88±1.37
0.015	80.5±2.5	12.95±0.85
0.020	86.1±3.0	13.49±1.0

Electrical Conductivity. Figure 2 shows the results of the electrical conductivity measurements. The conductivity decreases with increasing oxygen partial pressure. This result indicates that $BaFe_2O_4$ is an oxygen deficient, n-type oxide and that the dependence of conductivity on the oxygen pressure is given by $\sigma = P_{O_2}^{-1/m'}$. The values of m' are given in the third column of Table 1. The values are scattered with the mean value being 6.1.

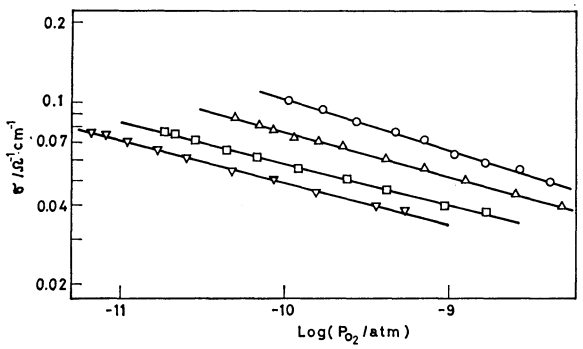

Fig. 2. Dependence of conductivity on oxygen partial pressure.

From the temperature dependence of the conductivity, the apparent activation energy for electronic conduction was calculated for a fixed composition. The results are given in the third column of Table 2. Although the standard deviations are relatively large, it appears that the apparent activation energy is independent of composition. The mean value is 12.7 kcal/mol.

Defect Models and the Expected Pressure Dependence of δ and σ. Measurements on nonstoichiometry and electrical conductivity have revealed that the dependence of the nonstoichiometry on oxygen partial pressure is different from that of the electrical conductivity, that is, the oxygen-pressure dependence is $P_{O_2}^{-1/2.88}$ for nonstoichiometry and $P_{O_2}^{-1/6.1}$ for conductivity. In order to interpret the difference in oxygen-pressure dependence consistently, a thermodynamic calculation was carried out on the defect concentration of oxygen deficit, n-type oxides on the basis of several defect models and the calculated results were compared with the data.

Interstitial cation models cannot be used to interpret the oxygen-pressure dependence, so oxygen vacancy models were examined. If V_0^x, $V_0^\cdot$, and $V_0^{\cdot\cdot}$ represent the neutral oxygen vacancy, the oxygen vacancy associated with one electron, and an oxygen vacancy free of electrons, respectively, the chemical equilibria relevant to these vacancies can be written as follows:

$$\text{null} = (1/2)O_2(g) + V_0^x,\ K_1 = [V_0^x]P_{O_2}^{1/2}, \quad (2)$$

$$V_0^x = V_0^{\cdot\cdot} + 2e',\ K_2 = n^2[V_0^{\cdot\cdot}]/[V_0^x], \quad (3)$$

$$V_0^x = V_0^\cdot + e',\ \text{and}\ K_3 = n[V_0^\cdot]/[V_0^x], \quad (4)$$

where K_1, K_2, and K_3 are equilibrium constants, the brackets express the concentration of the respective oxygen vacancies in units of moles per mole of $BaFe_2O_{4-\delta}$ and n is the concentration of electrons in the same units. The electrical neutrality condition is

$$n = 2[V_0^{\cdot\cdot}] + [V_0^\cdot]. \quad (5)$$

The nonstoichiometry, δ, and electrical conductivity, σ, are related to the oxygen-vacancy concentrations by

$$\delta = [V_0^x] + [V_0^\cdot] + [V_0^{\cdot\cdot}] \quad (6)$$

and

$$\sigma = (N_A/V_m)ne\mu = kn, \quad (7)$$

where V_m is the molar volume of $BaFe_2O_{4-\delta}$, N_A the Avogadro number, e the electronic charge, and μ the electron mobility. k is substituted for $(N_A/V_m)eu$ for the sake of simplification.

In the following, several defect models and the results of thermodynamic calculations on the basis of these models are described.

For the "A" models, one of the three kinds of oxygen vacancies are assumed to be predominant. If $V_0^\cdot$ is predominant, the elimination of V_0^x and $V_0^{\cdot\cdot}$ in Eqs. 5 and 6 and combining Eqs. 2, 4, 5, and 6 result in a relation whereby both δ and σ depend on $P_{O_2}^{-1/4}$. Let us call this the "A-2" model. Two other models, "A-1" and "A-3", are also proposed. The oxygen-pressure dependence of δ and σ for the "A" models is summarized in the first three lines of Table 3.

For the "B" models, two of the three kinds of oxygen vacancies are assumed to be predominant. Three models, "B-1", "B-2", and "B-3", and the oxygen-pressure dependence of δ and σ are as shown in the fourth to sixth lines of Table 3.

All three kinds of oxygen vacancies are assumed to prevail for the "C" model. The oxygen-pressure dependence of δ and σ is given in the last line of Table 3.

The observed pressure dependence is $P_{O_2}^{-1/2.88}$ for δ and $P_{O_2}^{-1/6}$ for σ. Therefore, two kinds of models, "B-3" and "C", appear to be appropriate for interpreting the observed results.

Thermodynamic Calculations on the Basis of the "C" Model. Equation 2 gives the concentration of V_0^x as

Table 3. Models and oxygen-pressure dependence

Model		Condition	Oxygen-pressure dependence m[a)]	m'[b)]
A	A-1	$[V_O^x] \gg [V_O^{\cdot}], [V_O^{\cdot\cdot}]$	2	
	A-2	$[V_O^{\cdot}] \gg [V_O^x], [V_O^{\cdot\cdot}]$	4	4
	A-3	$[V_O^{\cdot\cdot}] \gg [V_O^x], [V_O^{\cdot}]$	6	6
B	B-1	$[V_O^x], [V_O^{\cdot}] \gg [V_O^{\cdot\cdot}]$	2—4	4
	B-2	$[V_O^{\cdot}], [V_O^{\cdot\cdot}] \gg [V_O^{\cdot}]$	4—6	4—6
	B-3	$[V_O^x], [V_O^{\cdot\cdot}] \gg [V_O^{\cdot}]$	2—6	6
C		$[V_O^x] \approx [V_O^{\cdot}] \approx [V_O^{\cdot\cdot}]$	2—6	4—6

a) m is from $\delta \propto P_{O_2}^{-1/m}$. b) m' is from $\sigma \propto P_{O_2}^{-1/m'}$.

$$[V_O^x] = K_1 P_{O_2}^{-1/2}. \tag{8}$$

From Eqs. 3, 4, and 7,

$$[V_O^{\cdot}] = K_3[V_O^x]/n = K_1K_2kP_{O_2}^{-1/2}\sigma^{-1}, \tag{9}$$

$$[V_O^{\cdot\cdot}] = K_2[V_O^x]/n^2 = K_1K_3k^2P_{O_2}^{-1/2}\sigma^{-2}, \tag{10}$$

and, therefore,

$$P_{O_2}^{1/2} = K_1 + K_1K_3k\sigma^{-1} + K_1K_2k^2\sigma^{-2}. \tag{11}$$

Employing the observed values of δ, σ, and P_{O_2}, a least-squares calculation was carried out for Eq. 11, but no equilibrium constants simultaneously satisfying Eq. 11 could be found. Thus, "C" model was excluded from consideration and a detailed examination of the "B-3" model was carried out.

Thermodynamic Calculations on the Basis of the "B-3" Model. Omitting $[V_O^{\cdot}]$ in the right-hand side of Eq. 5, we obtain the neutrality condition,

$$n = 2[V_O^{\cdot\cdot}]. \tag{12}$$

Combination of Eqs. 2, 3, 7, and 12 yields

$$\sigma = (2K_1K_2k^3)^{1/3}P_{O_2}^{-1/6}. \tag{13}$$

Figure 3 shows a σ-$P_{O_2}^{-1/6}$ plot for the observed data. It is seen that Eq. 13 holds for the oxygen-pressure dependence of the conductivity. The concentrations of $V_O^{\cdot\cdot}$ and V_O^x can be expressed in terms of σ using Eqs. 2, 3, 7, and 12 as follows:

$$[V_O^{\cdot\cdot}] = n/2 = \sigma/2k \tag{14}$$

and

$$[V_O^x] = n^2[V_O^{\cdot\cdot}]/K_2 = \sigma^3/2K_2k^3. \tag{15}$$

Inserting Eqs. 14 and 15 into Eq. 6, and omitting $[V_O^{\cdot}]$, we obtain

$$2\delta/\sigma = 1/k + \sigma^2/K_2k^3. \tag{16}$$

This equation implies that a plot of $2\delta/\sigma$ against σ^2 would give a straight line and the value of k and the equilibrium constant K_2 could then be determined from the intercept and the slope of the line. Figure 4 shows a plot of $2\delta/\sigma$ *vs.* σ^2. Evidently, the data at constant temperature fall along a straight line. This result supports the "B-3" model.

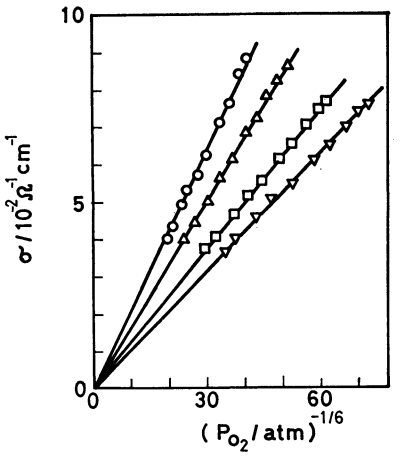

Fig. 3. The plot of σ against $P_{O_2}^{-1/6}$.

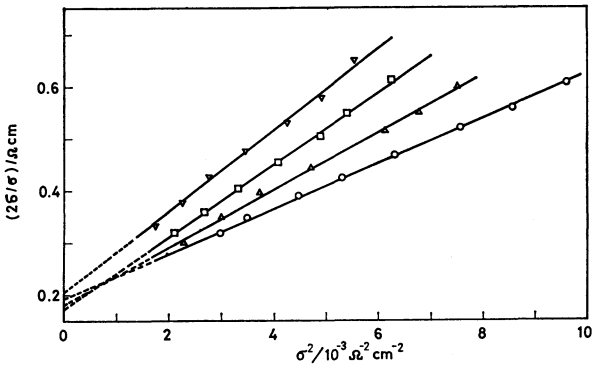

Fig. 4. The plot of $2\delta/\sigma$ against σ^2.

The k value calculated from the intercept is given in the second column of Table 4. The value of k appears to be independent of temperature in the temperature range between 1052 and 1125 °C. The average of k in this temperature range was 5.3 ± 0.4 cm^{-1} Ω^{-1}. From this value, the electron mobility was evaluated to be $(3.9\pm0.3)\times10^{-3}$ cm^2 V^{-1}.

The slope is listed in the third column of Table 4. The equilibrium constants, K_2, calculated from the slope and k are given in the fourth column of Table 4. Equa-

Table 4. Calculation of equilibrium constants, K_1 and K_2

t / °C	k / cm^{-1} Ω^{-1}	$1/(K_2k^3)$ / cm^3 Ω^3	K_2 / 10^{-5}	$2K_1K_2k^3$ / 10^{-10} atm$^{1/2}$ cm^{-3} Ω^{-3}	K_1 / 10^{-8} atm$^{1/2}$
1050	4.8±0.2	78±2	8.6±1.4	8.9±0.7	3.5±0.4
1075	5.8±0.2	69±1	9.7±1.0	19.1±0.6	6.6±0.3
1100	5.5±0.2	55±2	12.3±1.9	46.3±0.8	12.6±0.6
1125	5.1±0.1	43.0±0.3	15.6±0.2	95.1±0.7	20.5±1.6
	average: 5.3±0.4				
$\Delta S°$/cal mol^{-1}			3.8±2.4		32.1±2.2
$\Delta H°$/kcal mol^{-1}			29.7±3.3		87.5±2.2

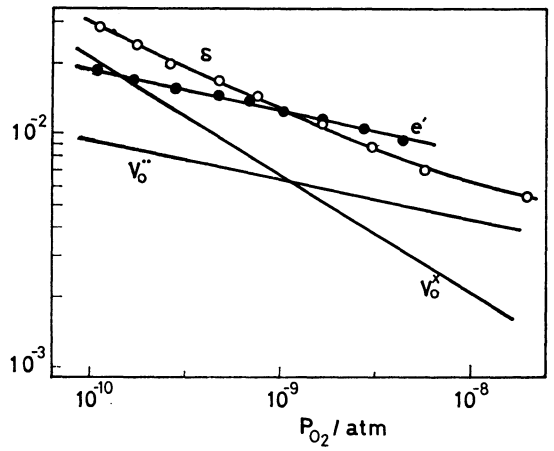

Fig. 5. Concentration of point defects in $BaFe_2O_{4-\delta}$ at 1125 °C.
○: δ, ●: concentration of conduction electron.

tion 13 indicates that the slope of the σ-$P_{O_2}^{-1/6}$ plot gives the value of $2K_1K_2k^3$, which is presented in the fifth column of Table 4. From this value and the slope obtained from Fig. 4, the equilibrium constant K_1 was calculated. The results are given in the last column of Table 4.

The concentrations of the lattice defects, V_O^x, $V_O^{\cdot\cdot}$ and electrons, and the nonstoichiometry, δ, were calculated from the values of K_1 and K_2 in Table 4. They are plotted together with δ in Fig. 5. The open circles designate the observed nonstoichiometric data and the solid circles designate the electron concentration calculated from the observed concentration data and the value of the electron mobility (3.9×10^{-3} cm^2 V^{-1}). It is seen that the oxygen vacancies V_O^x tend to dissociate into $V_O^{\cdot\cdot}$ and electrons as the oxygen partial pressure increases. The agreement is very good for both the electron concentration and the nonstoichiometry. Thus, the "B-3" model explains well the observed results.

The temperature dependence of the equilibrium constants, K_1 and K_2, can be represented by

$$K = \exp(\Delta S^\circ/R)\exp(-\Delta H^\circ/RT). \quad (17)$$

The values of ΔH° and ΔS° with one standard deviation are indicated in Table 4. The enthalpy change for Eq. 2 is 87.5 kcal/mol and that for Eq. 3 is 29.7 kcal/mol.

From these results it is concluded that the "B-3" model is best of those listed in Table 3 for interpreting the observed data for δ and σ.

References

1) F. A. Kroeger, "The Chemistry of Imperfect Crystals," North Holland Publ. Co., Amsterdam (1974).
2) P. Kofstad, "Nonstoichiometry, Diffusion, and Electrical Conductivity in Binary Metal Oxides," John Wiley, New York (1972).
3) L. Eyring and M. O'Keefe, eds., "The Chemistry of Extended Defects in Non-Metallic Solids," North Holland Publ. Co., Amsterdam (1970).
4) H. Schmalzried and C. Wagner, *Z. Phys. Chem. (Frankfurt am Main)*, **B31**, 198 (1962).
5) A. M. J. H. Seuter, *Philips Res. Rept.*, Suppl. No. 3 (1974).
6) S. A. Long and R. N. Blumenthal, *J. Am. Ceram. Soc.*, **54**, 610 (1971).
7) S. Meriani, *Acta Crystallogr., Sect. B*, **28**, 1241 (1972).
8) A. Nakamura, S. Yamauchi, K. Fueki, and T. Mukaibo, submitted to the *J. Phys. Chem. Solids.*
9) K. Endo, S. Yamauchi, K. Fueki, and T. Mukaibo, *J. Solid State Chem.*, **19**, 13 (1976).